Giant Anisotropic Magnetoresistance due to Purely Orbital Rearrangement in the Quadrupolar Heavy Fermion Superconductor PrV_2Al_{20}

Yasuyuki Shimura,[1,2,*] Qiu Zhang,[3] Bin Zeng,[3] Daniel Rhodes,[3] Rico Schönemann,[3] Masaki Tsujimoto,[1] Yosuke Matsumoto,[4] Akito Sakai,[1] Toshiro Sakakibara,[1] Koji Araki,[5] Wenkai Zheng,[3] Qiong Zhou,[3] Luis Balicas,[3] and Satoru Nakatsuji[1,6,†]

[1]*Institute for Solid State Physics, The University of Tokyo, Kashiwa, Chiba 277-8581, Japan*
[2]*Graduate School of Advanced Sciences of Matter, Hiroshima University, Higashi-Hiroshima 739-8530, Japan*
[3]*National High Magnetic Field Laboratory, Florida State University, Tallahassee, Florida 32310, USA*
[4]*Department of Quantum Materials, Max Planck Institute for Solid State Research, Heisenbergstrasse 1, Stuttgart 70569, Germany*
[5]*Department of Applied Physics, National Defense Academy, Yokosuka, Kanagawa 239-8686, Japan*
[6]*CREST, Japan Science and Technology Agency (JST), 4-1-8 Honcho Kawaguchi, Saitama 332-0012, Japan*

(Received 23 January 2019; published 25 June 2019)

We report the discovery of giant and anisotropic magnetoresistance due to the orbital rearrangement in a non magnetic correlated metal. In particular, we measured the magnetoresistance under fields up to 31.4 T in the cubic Pr-based heavy fermion superconductor PrV_2Al_{20} with a non magnetic Γ_3 doublet ground state, exhibiting antiferroquadrupole ordering below 0.7 K. For the [100] direction, we find that the high-field phase appears between 12 and 25 T, accompanied by a large jump at 12 T in the magnetoresistance ($\Delta MR \sim 100\%$) and in the anisotropic magnetoresistivity ratio by ~20%. These observations indicate that the strong hybridization between the conduction electrons and anisotropic quadrupole moments leads to the Fermi surface reconstruction upon crossing the field-induced antiferroquadrupole (orbital) rearrangement.

DOI: 10.1103/PhysRevLett.122.256601

Spintronic devices using both electronic charge and spin degrees of freedom (d.o.f.) have been developed, for instance, memory devices using the giant magnetoresistance effect of ferromagnetic multilayers [1]. In addition to the spin and charge d.o.f., electronic orbital d.o.f. have attracted much attention due to the discoveries of exotic orbital ordering and orbital liquid states [2,3]. Moreover, since electronic orbitals coupling with lattice are responsible for forming the band structure, the orbital rearrangement should make dramatic effects on the transport phenomena. Indeed, some perovskite-type manganese (Mn) oxides exhibit a gigantic negative magnetoresistance named as colossal magnetoresistance, induced by the suppression of the Mn orbital ordering under magnetic field [4].

On the other hand, to develop a higher density memory device, it is important to find a mechanism for non-ferromagnetic materials to exhibit a large transport anomaly such as anisotropic magnetoresistance (AMR) and anomalous Hall effect without having spontaneous magnetization, as they do not possess stray fields perturbing neighboring cells [5–7]. The AMR is defined as the difference between the resistances measured with currents applied parallel and perpendicular to the ordered spin direction. The AMR has been observed in the ferromagnetic and antiferromagnetic alloys [8]. In the case of antiferromagnets, the AMR effect has been limited to 1%–2% at room temperature [9,10]. Orbital ordering might be more useful for the observation of a large AMR not only because it should introduce anisotropy in the transport and in the electronic structure but also because orbital moments are in principle non magnetic. In fact, strongly anisotropic transport has been reported near the putative quantum critical point of the orbital (nematic) ordering in the iron-based superconductors [11–13].

In $3d$ transition metal compounds, however, the AMR may arise from various effects accompanied by the orbital ordering. First of all, the orbital ordering in the $3d$ systems is often induced by Jahn-Teller distortions, and thus the lattice distortion could lead to a large anisotropy in the resistance [14]. Furthermore, the orbital d.o.f. cannot be decoupled from the spin d.o.f.; thus, it is usually hard to neglect the magnetic contributions to the transport anisotropy [15]. Very interestingly, the transition metal oxides are often characterized by a spatially inhomogeneous state with a short mean free path, which may obscure the intrinsic effects due to orbital ordering [16].

In sharp contrast, the strong spin-orbit coupling in $4f$ rare-earth materials may provide an ideal situation for the study of orbital physics. For example, purely orbital effects can be studied in a cubic system that possesses non-Kramers rare-earth ions with even numbers of $4f$ electrons such as Pr^{3+}. Some of them exhibit a non magnetic Γ_3 doublet ground state stabilized by the cubic crystalline-electric field for the non-Kramers ions [17]. The Γ_3 doublet has only non magnetic electric quadrupole O_2^2, O_2^0, and octupole T_{xyz} moments, without magnetic dipole moments. Normally, these d.o.f. are lost at low temperatures by

multipole ordering. Moreover, compared to the transition metal systems, $4f$-electron systems have relatively low energy scales, and it is feasible to tune their ground states by external fields and pressure through quantum critical points [18–20].

The cubic Pr-based compound PrV_2Al_{20} has the Γ_3 ground doublet and exhibits antiferroquadrupole ordering below 0.6–0.7 K [21]. In the related compound $PrTi_2Al_{20}$, the Γ_3 ground doublet in the cubic crystalline electric field has been confirmed by inelastic neutron scattering measurements [22]. The analysis based on the cubic structure in PrV_2Al_{20} determined by the synchrotron x-ray diffraction study confirms Γ_3 ground doublet [23]. Within the quadrupolar ordered state, PrV_2Al_{20} undergoes a transition into a heavy fermion superconducting phase below 0.05 K, demonstrating the strong hybridization between conduction electrons and the quadrupole moments [24]. This strong hybridization has been also confirmed by various experimental probes, for instance, hyperfine coupling constant of Al nucleus as seen in the nuclear magnetic resonance measurement, thermoelectric power, and cyclotron effective mass detected by quantum oscillation in the magnetoresistance observed around [111] field direction [25–28]. In particular, the emergence of the quantum oscillation indicates that PrV_2Al_{20} is an intrinsically highly pure system without spatial inhomogeneity. In addition, the strong hybridization drives the system close to a quadrupolar quantum critical point. In fact, under magnetic fields along the [111] field direction, quantum critical behavior in the temperature dependence of the resistivity was observed around 11 T, where the quadrupole phase becomes fully suppressed [27]. On the other hand, field-induced exotic phenomena due to quadrupolar fluctuations are expected for other field directions. Along the [100] field direction, another high-field phase was found above 11–12 T below ~1 K via low-temperature magnetization measurements [29]. This high-field phase transition may well be induced by a rearrangement of quadrupole moments from the low-field antiferro ordered state. Given the large hybridization, the presence of the anisotropic magnetoresistance across the quadrupolar transition is highly likely and it is thus quite interesting and important to study the magnetoresistance effects of PrV_2Al_{20} under the field along [100].

In this Leter, we report comprehensive results of the magnetoresistance measurements and the magnetic phase diagram of the quadrupolar ordered state in PrV_2Al_{20} for the field parallel to the [100] direction. Especially, we have discovered a sharp magnetoresistive jump accompanied by a large AMR through the field-induced transition at 12 T for $B \parallel [100]$. The large and anisotropic magnetoresistance has never been reported for non magnetic quadrupolar systems. We attribute it to the reconstruction of the $4f$ Fermi surface caused by the field-induced switching of the quadrupole order. The experimental method is described in the Supplemental Material (SM) [30].

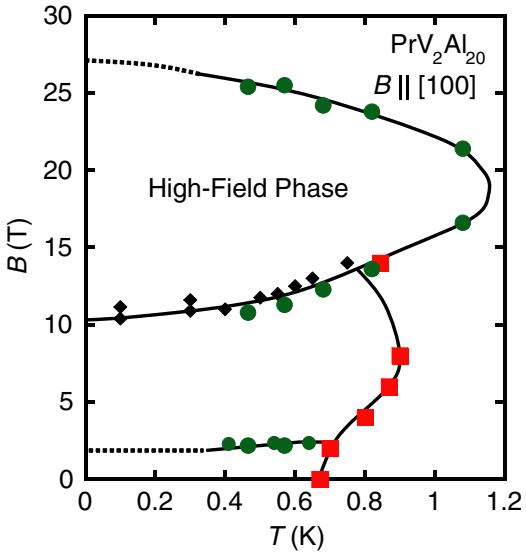

FIG. 1. B-T phase diagram for $B \parallel [100]$ obtained from the magnetoresistance $\rho(T, B)$. Circles indicate anomalies observed in $\rho(B)$, shown by open arrows in Fig. 2. Squares indicate the shoulder in $\rho(T)$ given in the Supplemental Material [30]. Diamonds are plotted from the anomalies in the low-temperature magnetization $M(B, T)$ [29].

First, as a summary, we present the magnetic phase diagram for $B \parallel [100]$ in Fig. 1, determined by the anomalies observed in the magnetoresistance $\rho(T, B)$. The reentrant character of the magnetic phase diagram (seen below 10 T in Fig. 1) is generally found in the antiferroquadrupole ordered systems. The high-field phase was observed between ~12 T and ~24 T below ~1.2 K. This phase cannot be explained by the crossing of the crystalline-electric-field levels since the magnitude of the gap (~40 K) between first-excited Γ_5 triplet and ground Γ_3 doublet is too large for such a level crossing [21,29,33]. For another cubic Γ_3 compound $PrPb_3$, Sato *et al.* has proposed a mechanism for the field-induced phase transition in the antiferroquadrupole ordered system with a Γ_3 ground doublet for $B \parallel [100]$ [34]. Accordingly, an antiferroquadrupole O_2^2 state is also expected to become stable under high $B \parallel [100]$ assisted by the octupole T_β interaction. As we show below and in the SM, the sharp anomalies seen in the field and temperature dependences of the resistivity across the phase boundaries into the high-field phase and the near absence of a corresponding change in the magnetization indicate that the high-field phase should be indeed an antiferroquadrupole state.

Figure 2 shows the field dependence of the magnetoresistance $\rho(B)$ for $B \parallel [100]$ ($\perp I \parallel [011]$) below 1.3 K up to 31.4 T. At 0.46 K, we observed three anomalies, the shoulder at 2 T, a distinct jump with a hysteresis at 12 T and a kink at 25 T. As shown in the inset, a shoulder at ~2 T does not exhibit clear temperature dependence up to $T_Q \sim 0.64$ K. The jump at 12 T indicates the transition

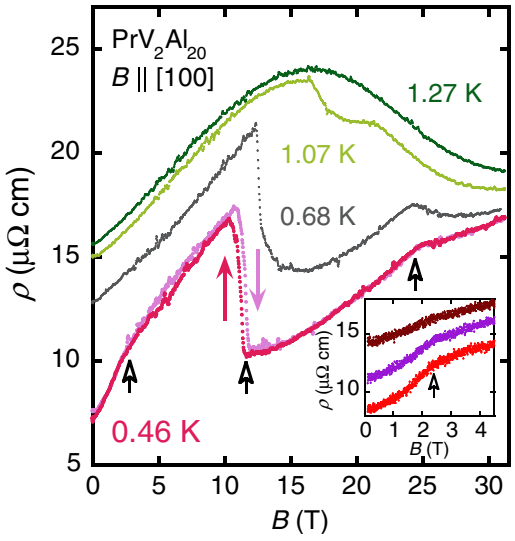

FIG. 2. Field dependence of the magnetoresistance $\rho(B)$ for $B \parallel [100]$ below ~1.3 K up to 31.4 T. The inset shows $\rho(B)$ below 4.5 T measured at 0.41 K (red), 0.54 K (purple), and 0.64 K (brown). The open arrows denote the transition fields.

to the high-field phase as observed in the low-temperature magnetization measurements [29]. The hysteresis observed at 0.46 K indicates the first-order character of this transition. With increasing temperature, two anomalies at 12 and 25 T approach each other and disappear at 1.27 K. In the SM, we show the temperature dependence of the resistivity $\rho(T)$ under fields up to 28 T for $B \parallel [100]$ [30]. In the temperature dependence, the kinks due to the transitions for low- and high-field phases are also detected. Note that the resistivity anomalies across the phase boundary into the high-field phase are sharp. This clearly indicates that the high-field phase should not be a ferro- but an antiferroquadrupole order, as we discussed above. From these anomalies in $\rho(T, B)$, the multiple phase diagram is constructed as shown in Fig. 1. Above ~25 T, we did not detect any anomalies in both $\rho(B)$ and $\rho(T)$, indicating that, for fields above 25 T, one stabilizes polarized paraquadrupole states.

As shown in Fig. 2, we find a large magnetoresistance jump across the field-induced transition at 12 T for $B \parallel [100]$. The magnitude of the change of the magnetoresistance at the transition is $\Delta MR = \Delta\rho_{\rm jump}/\rho_{0\rm T} \sim 100\%$. Both data for increasing and decreasing field sweep of $\rho(B)$ at 0.46 K in the high-field phase overlap on top of each other. This indicates the magnetoresistance in the high-field phase is not due to spatial inhomogeneity. We note this giant jump in $\rho(B)$ is observed only for the case of $B \parallel [100]$ among all the transverse magnetoresistance measurements ($B \perp I \parallel [011]$, see SM) taken under fields B along the three cubic principal directions. As we discussed, a similar high-field phase for $B \parallel [100]$ was also observed in the cubic antiferroquadrupole ordered system $PrPb_3$ with the Γ_3 ground doublet [34]. However, the magnetoresistance anomaly due to the field-induced phase transition in $PrPb_3$ is much smaller than our data for PrV_2Al_{20} [35]. The important character peculiar to PrV_2Al_{20} is the strong hybridization between conduction electrons and quadrupole moments. Indeed, the quadrupolar fluctuation is enhanced by the strong magnetic field as discussed for $B \parallel [111]$ [27]. Thus, the field-induced quadrupole rearrangement most likely causes a reconstruction of the parts of the Fermi surface that have a large $4f$ contribution through the strong hybridization, thus resulting in the large change in the magnetoresistance.

Since a quadrupole moment results from an anisotropic charge distribution, the band structure and the resultant transport properties should also become anisotropic by the quadrupole ordering. In order to evaluate the anisotropy, we focus on the anisotropic magnetoresistance (AMR) ratio in the high-field phase above 12 T for $B \parallel [100]$. AMR is defined as the difference between the longitudinal magnetoresistance $\rho_{\parallel}$ and the transverse magnetoresistance $\rho_{\perp}$.

Figures 3(a) and 3(b) show the magnetoresistance for two conditions of $B \parallel I \parallel [100]$ (longitudinal, $\rho_{\parallel}$) and $B \parallel [010]$ $\perp I \parallel [100]$ (transverse, $\rho_{\perp}$) at 0.45 and 1.6 K, respectively. We also measured them in the reference compound LaV_2Al_{20} without $4f$ electrons. Since these have a cubic crystal structure, the electronic state for $B \parallel [100]$ is intrinsically the same as that for $B \parallel [010]$. Therefore, we may study the longitudinal and transverse magnetoresistance without changing the electronic state even under magnetic field. Longitudinal and transverse conditions for the same sample were obtained by rotating the sample holder. These two field angles are precisely determined by the Hall sensors attached to the sample holder at low temperatures. At 0.45 K inside the ordered phase in PrV_2Al_{20}, we observe two anomalies at 12 and 23 T, which are almost consistent with those found in the magnetoresistance shown in Fig. 2.

Figure 3(c) shows the AMR ratio $(\rho_{\perp} - \rho_{\parallel})/\rho_{\rm av}$, where $\rho_{\rm av} = (2\rho_{\perp} + \rho_{\parallel})/3$, obtained from the data given in Figs. 3(a) and 3(b). In the high-field phase in PrV_2Al_{20}, the value of AMR is about 30%. The large AMR with evident anomalies at 12 and 23 T, is consistent with those in the phase boundary in Fig. 1, and disappears in the paraquadrupole state at 1.6 K, indicating that this large AMR arises from the static ordered state. AMR in the reference compounds LaV_2Al_{20} without $4f$ electrons is only 5%–10% in this field region. These indicate that 20%–25% AMR in the high-field phase in PrV_2Al_{20} is purely due to the $4f$ contribution. From these, the large AMR in the high-field phase in PrV_2Al_{20} cannot be explained by the cyclotron motion inducing the transverse magnetoresistance.

To discuss the origin of the AMR in the high-field phase, we examine the field dependence of the linear magnetostriction $\Delta L/L_0$ and of the magnetization M at 0.1 K up to 14.5 T for $B \parallel [100]$, where L_0 is the sample size at room temperature. The magnetization data were already reported

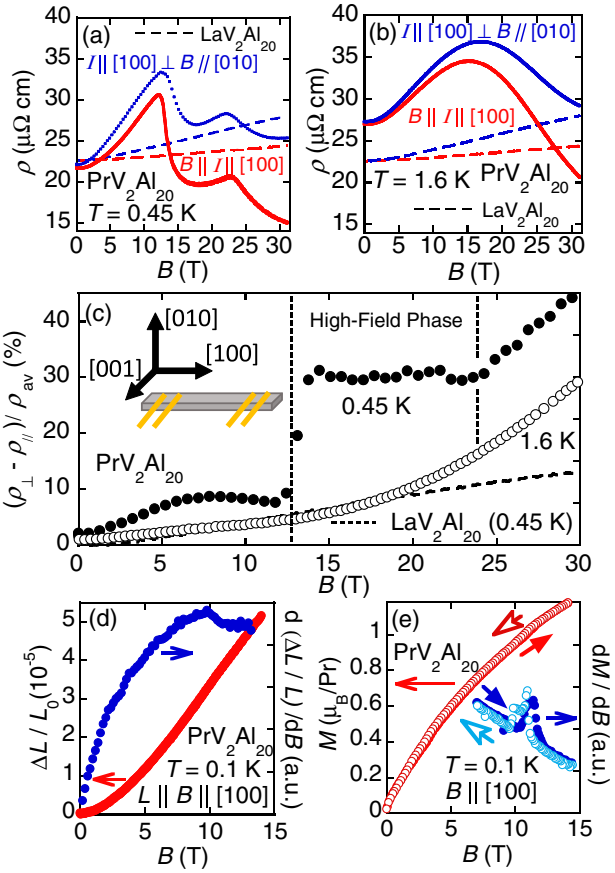

FIG. 3. Longitudinal and transverse magnetoresistance for $B \parallel I \parallel [100]$ and $B \parallel [010] \perp I \parallel [100]$ at 0.45 K (a) and 1.6 K (b) up to 31 T in PrV_2Al_{20}, respectively. Dashed line indicates those in LaV_2Al_{20}. (c) displays the anisotropic magnetoresistance ratio $(\rho_\perp - \rho_{||})/\rho_{\rm av}$, where $\rho_{\rm av} = (2\rho_\perp + \rho_{||})/3$, obtained from the data in (a) and (b). (d) indicates the linear magnetostriction $\Delta L/L_0$ for $L \parallel B \parallel [100]$ up to 14.5 T and $(d\Delta L/L_0)/dB$ at 0.1 K. (e) displays the magnetization M for $B \parallel [100]$ up to 14.5 T and dM/dB at 0.1 K [29].

in Ref. [29]. The field derivatives $d\Delta L/L_0/dB$ and dM/dB exhibit tiny but distinct anomalies at ~12 T due to the crossing of the phase boundary towards the high-field phase. The clear jump in AMR ratio (20%–25%) is much different from the field dependence of $\Delta L/L_0$ and M. This weak anomaly in M and $\Delta L/L_0$ suggests that the AMR in the high-field phase is not accompanied by any macroscopic lattice distortion and magnetization change. Around 12 T, the magnitude of the tiny metamagnetic jump is just 0.6% of $3.2\mu_B$, the full moment of Pr^{3+}. The value of $\Delta L/L_0$ at 12 T is just 0.005%, suggesting the cubic structure is almost preserved even in the high-field phase. The AMR with almost no spontaneous magnetization change and distortion in the high-field phase probably comes from the non magnetic field-induced antiferroquadrupole ordering strongly coupling with the conduction electrons. In comparison, the AMR ratio in antiferromagnetic materials has been limited to 1%–2% which is 1 order magnitude smaller than our observations [9,10].

In the Supplemental Material [30], we further provide the detailed results of anisotropic magnetoresistance for different crystallographic axes, which indicates that the observed AMR is due to the $4f$ quadrupole moments. First, the field-angular dependence has far more fine structure than the ellipsoidal angle dependence seen in the transition metal oxides with spatial inhomogeneity, for example, in the Mn oxides with inhomogeneous charge ordering [14,16]. In contrast, we find no sharp jump in $\rho(B)$ and a much weaker enhancement of AMR for $B \parallel [110]$. For $B \parallel [111]$, it has been reported that the magnetic field suppresses the quadrupole order at 11 T and instead a polarized para-quadrupole state emerges above 11 T [27]. Thus, the high-field phase with the large AMR is unique for $B \parallel [100]$ among three cubic principal field directions. Numerical simulation assuming the quadrupole interaction in $Pr\,T_2X_{20}$ also points out that the antiferroquadrupole O_2^2 ordered state becomes stable only for $B \parallel [100]$ [36], which is consistent with our observations. At higher fields above 23 T, the large AMR remains and is rapidly enhanced with increasing magnetic field. This is due to the polarized quadrupole moments $O_2^0 = (3J_z^2 - J^2)/2$, which is expected to grow quadratically with the field, as the magnetization $\sim J_z$ increases linearly with the magnetic field. In contrast, the AMR in the low-field phase below 12 T is small. This implies that the anisotropy of the multipole order parameter is weaker than that under the higher field.

Thus, our experimental results can be naturally understood that the field-induced AMR originates from the antiferroquadrupole ordering, and thus cannot be simply accounted for by breaking of the discrete rotational symmetry due to electronic nematic state.

As has been discussed for RB_{12} (R = rare earth) exhibiting dynamic charge stripe, the observed anisotropic magnetoresistance would come from the intrinsic and/or extrinsic defects coupling with the low-symmetric ordered state [37–40]. To examine the possibility, we also show AMR in SM under the same field and current configuration for a low-quality sample whose drop in the resistivity by quadrupole transition at 0.6–0.7 K is not clearly observed. Both of the magnitude of the magnetoresistance jump and AMR in this low-quality sample are smaller than those, described in Figs. 3(a)–3(c), in the higher-quality sample exhibiting a clear quadrupole transition at zero field in the resistivity. These results suggest that the magnetoresistance jump and AMR are not due to the intrinsic and/or extrinsic defects in the crystals, but due to the quadrupole ordering in the bulk.

Finally, we compare our results for PrV_2Al_{20} with the case of iron-based superconductors $Ba(Fe_{1-x}Co_x)_2As_2$, which also exhibit a strongly anisotropic resistance almost without macroscopic distortion and spontaneous magnetization. In $BaFe_2As_2$, the antiferromagnetic ordering almost

coincides with a tetragonal to orthorhombic structural transition at 130 K [41]. By doping Co, these transition temperatures are strongly suppressed and disappear at the Co composition of $x \sim 0.07$, where the superconducting transition temperature peaks [42]. Significantly, in the low-temperature antiferromagnetic orthorhombic phase, the laser angle-resolved photoemission spectroscopy has revealed that the Fermi surface is mainly composed of iron $3d$ bands [11]. In the orthorhombic phase of $BaFe_2As_2$, the lattice parameters are $a = 5.615\,87$ Å, $b = 5.571\,25$ Å, and $c = 12.9428$ Å, almost preserving the tetragonal structure. Note that, at $x \sim 0.04$ in the vicinity of the composition ($x = 0.07$) where the structural transition disappears, the ab-plane anisotropy in the resistance strongly develops up to $\rho_{I||b}/\rho_{I||a} \sim 1.8$, where the anisotropic resistance ratio is $(\rho_{I||b} - \rho_{I||a})/\rho_{\rm ave} \sim 60\%$ [$\rho_{\rm ave} = (\rho_{I||b} + \rho_{I||a})/2$] [12]. Above the temperatures of structural transition and superconducting dome, an electronic nematic state with a local ab-plane anisotropy was revealed by angle-resolved magnetic torque and synchrotron x-ray measurements [13]. While there would still be some effects due to $3d$ spin correlations, these observations suggest that the ab-plane anisotropic resistance would originate from the electronic nematic order due to the $3d$ orbitals and not from a macroscopic structural distortion.

Very interestingly, a possible electronic nematicity has also been pointed out for the $4f$-electron-based tetragonal antiferromagnet $CeRhIn_5$ [43]. Namely, a substantial anisotropy in the ab-plane magnetoresistivity was observed in the vicinity of a field-induced antiferromagnetic quantum critical point, suggesting the emergence of the electronic nematic state [43]. The nematicity has also been suggested based on the angular dependence of the magnetoresistance in the antiferroquadrupole or magnetic ordered system CeB_6 with Γ_8 quartet ground state formed by two Kramers doublets. This nematicity is argued to be induced by the (magnetic) spin fluctuation [44]. However, in the above cases of Ce-based compounds as well as Fe-based superconductors, it is hard to isolate the pure orbital contribution to the magnetoresistance since the Ce ion has a net $4f$ moment due to the Kramers degeneracy.

Here, we note that our discovery in this Letter provides a much clearer case without involving any spin d.o.f. Namely, our observation of the large AMR in the high-field phase of PrV_2Al_{20} for B || [100] results from the spontaneous change in the c-f hybridized band structure induced by the rearrangement in the $4f$-non magnetic orbitals (quadrupoles). This orbital rearrangement causes almost no change in the magnetization or crystal structure. Finally, in order to confirm this scenario, theoretical studies based upon band structure calculations should be performed in the future.

In conclusion, we have measured the magnetoresistance in the cubic antiferroquadrupole ordered state of the heavy fermion superconductor PrV_2Al_{20} having a non magnetic quadrupolar doublet ground state and established the magnetic phase diagram for B || [100]. Upon entering the high-field phase at 12 T, we have discovered a large magnetoresistance jump with the magnetoresistance ratio 100% accompanied by the large change in the anisotropic magnetoresistance by ~20%. These large changes in the magnetoresistance and its anisotropy are the consequences of the reconstruction of the Fermi surface at the field-induced quadrupole rearrangement due to the strong hybridization between the conduction electrons and the non magnetic $4f$ quadrupole moments.

We thank K. Hattori, K. Matsubayashi, J. Suzuki, and Y. Uwatoko for useful discussions. This work is partially supported by CREST (JPMJCR15Q5, JPMJCR18T3), Japan Science and Technology Agency, Grants-in-Aid for Scientific Research (No. 25707030, No. 15J08663, and No. 25887015), by Grants-in-Aids for Scientific Research on Innovative Areas (15H05882, 15H05883), and the Program for Advancing Strategic International Networks to Accelerate the Circulation of Talented Researchers (No. R2604) from the Japanese Society for the Promotion of Science. Y. S. is partially supported by the Institute of Complex Adaptive Matter (ICAM). L. B. is supported by DOE-BES through Award No. DE-SC0002613. The NHMFL is supported by NSF through NSF-DMR-1157490 and the State of Florida.

*simu@hiroshima-u.ac.jp
†satoru@issp.u-tokyo.ac.jp

[1] M. N. Baibich, J. M. Broto, A. Fert, F. Nguyen Van Dau, F. Petroff, P. Etienne, G. Creuzet, A. Friederich, and J. Chazelas, Phys. Rev. Lett. **61**, 2472 (1988).
[2] Y. Tokura and N. Nagaosa, Science **288**, 462 (2000).
[3] S. Nakatsuji, K. Kuga, K. Kimura, R. Satake, N. Katayama, E. Nishibori, H. Sawa, R. Ishii, M. Hagiwara, F. Bridges, T. U. Ito, W. Higemoto, Y. Karaki, M. Halim, A. A. Nugroho, J. A. Rodriguez-Rivera, M. A. Green, and C. Broholm, Science **336**, 559 (2012).
[4] Y. Tokura, Rep. Prog. Phys. **69**, 797 (2006).
[5] S. Nakatsuji, N. Kiyohara, and T. Higo, Nature (London) **527**, 212 (2015).
[6] N. Kiyohara, T. Tomita, and S. Nakatsuji, Phys. Rev. Applied **5**, 064009 (2016).
[7] T. Jungwirth, X. Marti, P. Wadley, and J. Wunderlich, Nat. Nanotechnol. **11**, 231 (2016).
[8] T. McGuire and R. Potter, IEEE Trans. Magn. **11**, 1018 (1975).
[9] D. Kriegner, K. Vyborny, K. Olejnik, H. Reichlova, V. Novak, X. Marti, J. Gazquez, V. Saidl, P. Nemec, V. V. Volobuev, G. Springholz, V. Holy, and T. Jungwirth, Nat. Commun. **7**, 11623 (2016).
[10] X. Marti, I. Fina, C. Frontera, J. Liu, P. Wadley, Q. He, R. J. Paull, J. D. Clarkson, J. Kudrnovsky, I. Turek, J. Kunes, D. Yi, J.-H. Chu, C. Nelson, L. You, E. Arenholz, S. Salahuddin, J. Fontcuberta, T. Jungwirth, and R. Ramesh, Nat. Mater. **13**, 367 (2014).

[11] T. Shimojima, K. Ishizaka, Y. Ishida, N. Katayama, K. Ohgushi, T. Kiss, M. Okawa, T. Togashi, X.-Y. Wang, C.-T. Chen, S. Watanabe, R. Kadota, T. Oguchi, A. Chainani, and S. Shin, Phys. Rev. Lett. **104**, 057002 (2010).
[12] J.-H. Chu, J. G. Analytis, K. De Greve, P. L. McMahon, Z. Islam, Y. Yamamoto, and I. R. Fisher, Science **329**, 824 (2010).
[13] S. Kasahara, H. J. Shi, K. Hashimoto, S. Tonegawa, Y. Mizukami, T. Shibauchi, K. Sugimoto, T. Fukuda, T. Terashima, A. H. Nevidomskyy, and Y. Matsuda, Nature (London) **486**, 382 (2012).
[14] R.-W. Li, H. Wang, X. Wang, X. Z. Yu, Y. Matsui, Z.-H. Cheng, B.-G. Shen, E. W. Plummer, and J. Zhang, Proc. Natl. Acad. Sci. U.S.A. **106**, 14224 (2009).
[15] H. Kuwahara, T. Okuda, Y. Tomioka, A. Asamitsu, and Y. Tokura, Phys. Rev. Lett. **82**, 4316 (1999).
[16] E. Dagotto, Science **309**, 257 (2005).
[17] K. Lea, M. Leask, and W. Wolf, J. Phys. Chem. Solids **23**, 1381 (1962).
[18] H. v. Löhneysen, A. Rosch, M. Vojta, and P. Wölfle, Rev. Mod. Phys. **79**, 1015 (2007).
[19] P. Gegenwart, Q. Si, and F. Steglich, Nat. Phys. **4**, 186 (2008).
[20] S. Nakatsuji, K. Kuga, Y. Machida, T. Tayama, T. Sakakibara, Y. Karaki, H. Ishimoto, S. Yonezawa, Y. Maeno, E. Pearson, G. G. Lonzarich, L. Balicas, H. Lee, and Z. Fisk, Nat. Phys. **4**, 603 (2008).
[21] A. Sakai and S. Nakatsuji, J. Phys. Soc. Jpn. **80**, 063701 (2011).
[22] T. J. Sato, S. Ibuka, Y. Nambu, T. Yamazaki, T. Hong, A. Sakai, and S. Nakatsuji, Phys. Rev. B **86**, 184419 (2012).
[23] D. Okuyama, M. Tsujimoto, H. Sagayama, Y. Shimura, A. Sakai, A. Magata, S. Nakatsuji, and T. J. Sato, J. Phys. Soc. Jpn. **88**, 015001 (2019).
[24] M. Tsujimoto, Y. Matsumoto, T. Tomita, A. Sakai, and S. Nakatsuji, Phys. Rev. Lett. **113**, 267001 (2014).
[25] Y. Tokunaga, H. Sakai, S. Kambe, A. Sakai, S. Nakatsuji, and H. Harima, Phys. Rev. B **88**, 085124 (2013).
[26] Y. Machida, T. Yoshida, T. Ikeura, K. Izawa, A. Nakama, R. Higashinaka, Y. Aoki, H. Sato, A. Sakai, S. Nakatsuji, N. Nagasawa, K. Matsumoto, T. Onimaru, and T. Takabatake, J. Phys. Conf. Ser. **592**, 012025 (2015).
[27] Y. Shimura, M. Tsujimoto, B. Zeng, L. Balicas, A. Sakai, and S. Nakatsuji, Phys. Rev. B **91**, 241102(R) (2015).
[28] Y. Shimura, M. Tsujimoto, A. Sakai, B. Zeng, L. Balicas, and S. Nakatsuji, J. Phys. Conf. Ser. **592**, 012026 (2015).
[29] Y. Shimura, Y. Ohta, T. Sakakibara, A. Sakai, and S. Nakatsuji, J. Phys. Soc. Jpn. **82**, 043705 (2013).
[30] See Supplemental Material at http://link.aps.org/supplemental/10.1103/PhysRevLett.122.256601 for experimental methods and the detailed magnetoresistance data, which includes Refs. [31,32].
[31] M. Tsujimoto, Y. Matsumoto, and S. Nakatsuji, J. Phys. Conf. Ser. **592**, 012023 (2015).
[32] T. Tayama, Y. Isobe, T. Sakakibara, H. Sugawara, and H. Sato, J. Phys. Soc. Jpn. **78**, 044708 (2009).
[33] K. Araki, Y. Shimura, N. Kase, T. Sakakibara, A. Sakai, and S. Nakatsuji, J. Phys. Soc. Jpn. Conf. Proc. **3**, 011093 (2014).
[34] Y. Sato, H. Morodomi, K. Ienaga, Y. Inagaki, T. Kawae, H. S. Suzuki, and T. Onimaru, J. Phys. Soc. Jpn. **79**, 093708 (2010).
[35] T. Yoshida, Y. Machida, K. Izawa, T. Onimaru, and H. S. Suzuki, J. Phys. Conf. Ser. **683**, 012031 (2016).
[36] K. Hattori and H. Tsunetsugu, J. Phys. Soc. Jpn. **83**, 034709 (2014).
[37] N. Sluchanko, A. Bogach, N. Bolotina, V. Glushkov, S. Demishev, A. Dudka, V. Krasnorussky, O. Khrykina, K. Krasikov, V. Mironov, V. B. Filipov, and N. Shitsevalova, Phys. Rev. B **97**, 035150 (2018).
[38] N. B. Bolotina, A. P. Dudka, O. N. Khrykina, V. N. Krasnorussky, N. Y. Shitsevalova, V. B. Filipov, and N. E. Sluchanko, J. Phys. Condens. Matter **30**, 265402 (2018).
[39] N. E. Sluchanko, A. N. Azarevich, A. V. Bogach, N. B. Bolotina, V. V. Glushkov, S. V. Demishev, A. P. Dudka, O. N. Khrykina, V. B. Filipov, N. Y. Shitsevalova, G. A. Komandin, A. V. Muratov, Y. A. Aleshchenko, E. S. Zhukova, and B. P. Gorshunov, J. Phys. Condens. Matter **31**, 065604 (2019).
[40] N. E. Sluchanko, A. L. Khoroshilov, A. V. Bogach, V. V. Voronov, V. V. Glushkov, S. V. Demishev, V. N. Krasnorussky, K. M. Krasikov, N. Y. Shitsevalova, and V. B. Filipov, JETP Lett. **107**, 30 (2018).
[41] Q. Huang, Y. Qiu, W. Bao, M. A. Green, J. W. Lynn, Y. C. Gasparovic, T. Wu, G. Wu, and X. H. Chen, Phys. Rev. Lett. **101**, 257003 (2008).
[42] S. Nandi, M. G. Kim, A. Kreyssig, R. M. Fernandes, D. K. Pratt, A. Thaler, N. Ni, S. L. Bud'ko, P. C. Canfield, J. Schmalian, R. J. McQueeney, and A. I. Goldman, Phys. Rev. Lett. **104**, 057006 (2010).
[43] F. Ronning, T. Helm, K. R. Shirer, M. D. Bachmann, L. Balicas, M. K. Chan, B. J. Ramshaw, R. D. McDonald, F. F. Balakirev, M. Jaime, E. D. Bauer, and P. J. W. Moll, Nature (London) **548**, 313 (2017).
[44] S. V. Demishev, V. N. Krasnorussky, A. V. Bogach, V. V. Voronov, N. Y. Shitsevalova, V. B. Filipov, V. V. Glushkov, and N. E. Sluchanko, Sci. Rep. **7**, 17430 (2017).